Dynamic Hydraulic Fracture Modeling for Wellbore Integrity Prediction in a Porous Medium

Nikolay M. Kostov[1], Jing Ning[1], Shekhar V. Gosavi[2], Piyush Gupta[3], Kaustubh Kulkarni[1] and Pablo F. Sanz[1]

[1]ExxonMobil Upstream Research Company

[2]ExxonMobil Development Company

[3]ExxonMobil Upstream Research Company 2014 Summer Intern

Abstract: *We present a workflow for modeling dynamic growth of hydraulically induced fractures in a porous medium in the near-wellbore region. The focus is on the early time fracture growth behavior and the stress state near the wellbore as a result of it. The model is based on the Cohesive Zone Model (CZM) elements with pore pressure degrees of freedom, which were co-developed with ExxonMobil Upstream Research Company and recently implemented into the Abaqus finite element package. In addition to including the physics of dynamic fracture growth and pore pressure diffusion, the model allows for fluid leak-off from the wellbore and fracture faces into the porous medium, as well as an arbitrary injection schedule. The dynamic fracture growth and interaction between the stress concentration region near the tip and the wellbore result in a non-linear behavior of the near-wellbore stress state during early time fracture propagation. This analysis allows for a recommendation of optimum fracture width for a corresponding maximum increase in wellbore integrity for the target formation. The model also provides an effective tool to improve the treatment selection (e.g., particle size distribution for effective treatment), as well as field diagnostics for various lost circulation treatments and lost returns events. The model is incorporated into a fully automated workflow which allows the user to setup the analysis without any previous experience with Abaqus.*

Keywords*: CZM, drilling and subsurface, hydraulic fracturing, lost circulation, lost returns, oil and gas, wellbore integrity*

1. Introduction

Rotary drilling requires the use of a circulating fluid. While this fluid has a variety of vital roles, of particular importance is the ability to carry the formation cuttings, which are generated at the bit, to the surface. However, due to the hydrostatic head of the fluid at great depth and the dynamic pressure from the fluid motion, the forces acting on the wellbore faces can become high enough to induce mode I tensile fractures. When a large enough volume of fluid is lost to these fractures, the ability to carry the cuttings to the surface diminishes and this can prevent further drilling.

In this paper, we investigate the early time initiation and dynamic growth of such hydraulically induced fractures in a porous formation. The analysis of the changing width and length of the fracture and the changing stress state in the near-wellbore region can help us understand how to prevent such fractures. In addition, accurate prediction of the fracture geometry is important for the selection of the treatment needed to seal the fracture to prevent further drilling fluid loss.

We use a symmetric 2D plane strain model of the wellbore with Cohesive Zone Model (CZM) elements representing the induced fracture plane. This allows modeling the transient behavior of a bi-wing hydraulically induced mode I fracture in a porous medium while keeping the number of degrees of freedom manageable. This is of prime importance, as a large number of runs are required to evaluate different formation and fluid properties. We have developed an automated workflow which can generate the Abaqus input files, including an optimized mesh, execute the analysis and present the user with the post-processed results of interest.

Most of the results which these new Abaqus capabilities can generate have not been available through static analysis. The transient effects of the pore pressure diffusion and the interaction between the stress concentration around the moving fracture tip and the borehole all play a significant role on the tangential (hoop) stresses at the borehole face. The analysis results allow recommending the ideal fracture width at the mouth for which the tangential stresses around the borehole are maximized. This increase in stresses at the wellbore can prevent further fracture initiation.

Traditionally, there are two models used to estimate the wellbore pressure at which fracture initiation occurs from a wellbore in a porous medium. The first one is the Hubbert-Willis model (Equation 1) which considers the stress state around an infinite cylindrical borehole with two far field stresses and formation pore pressure acting on it, but does not consider the effect of fluid diffusion into the formation (Hubbert, 1957). The second one is the Haimson-Fairhurst model (Equation 2) which adds the steady state effect of increasing the near-wellbore pore pressure (Haimson, 1967). These are usually considered the upper and lower limit, respectively, for the fracture initiation pressure. However, because of uncertainties in the material properties and the irregularity of the borehole shape, often, more conservative estimates are used in practice.

$$P_i = T + 3\,\sigma_{\min} - \sigma_{\max} - P_p \qquad \text{Eq. 1}$$

$$P_i = \frac{T + 3\,\sigma_{\min} - \sigma_{\max} - 2\eta P_p}{2(1-\eta)} \qquad \text{Eq. 2}$$

Here P_i is the fracture initiation pressure (i.e., wellbore pressure at which fracture initiation occurs), T is the tensile strength of the rock, $\sigma_{\min}$ and $\sigma_{\max}$ are the minimum and maximum far field stresses, P_p is the initial pore pressure and $\eta=\alpha(1-2\nu)/2(1-\nu)$, with ν being the Poisson ratio and α the Biot parameter of the rock. A compression-positive sign convention is used for stresses and pressures.

A map of the fracture initiation pressure (nondimensionalized by $\sigma_{\min}$) as a function of the formation pore pressure (P_p) and the maximum far field stress ($\sigma_{\max}$) for each of the two models is shown in Figure 1.

While these two approaches give reasonable estimates for the fracture initiation pressure, they are still not capturing the time-dependent effects of fluid diffusion. More importantly, they do not provide any information about the fracture dimensions, or the wellbore stresses, once a fracture has been induced. To the authors' knowledge, there are no analytical models which can predict the near-wellbore stresses during fracture growth.

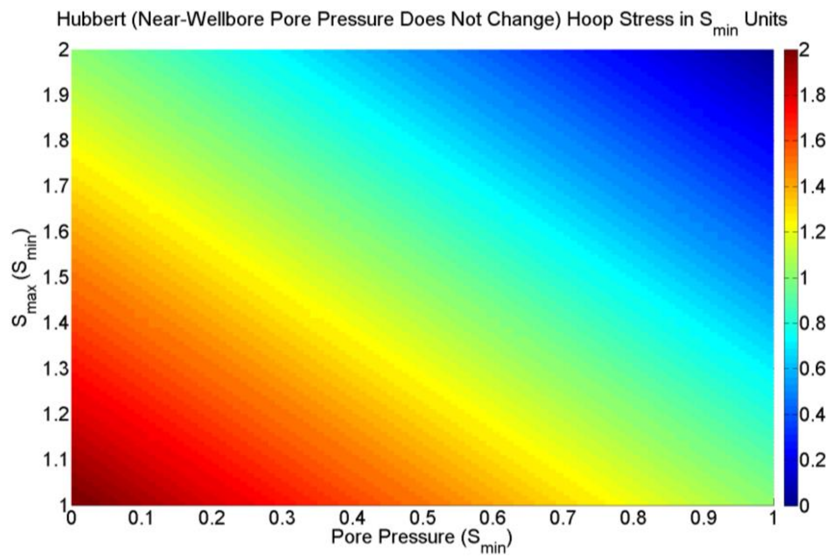

Hubbert-Willis Fracture Initiation Pressure nondimensionalized by σ_{min} as a function of pore pressure and maximum far field stress. We assume no tensile strength.

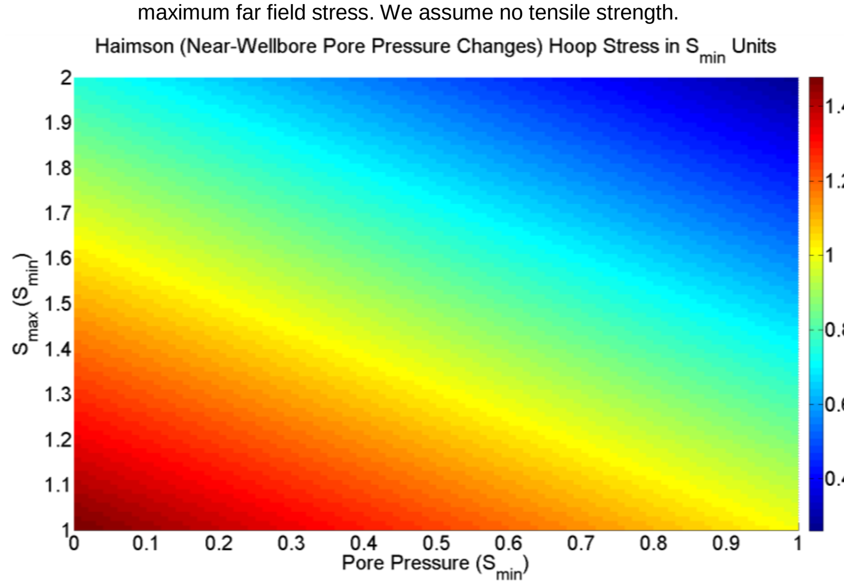

Haimson-Fairhurst Fracture Initiation Pressure nondimensionalized by σ_{min} as a function of pore pressure and maximum far field stress. We assume no tensile strength and η=0.3.

Figure 1. Hubbert-Willis (a) and Haimson-Fairhurst (b) models for fracture initiation

2. Model

The proposed method for modeling the stresses near the wellbore during the dynamic growth of the hydraulically induced fracture will be described next. ExxonMobil Upstream Research Company has been working with Simulia on developing new hydraulic fracturing capabilities into Abaqus. The coupled pore pressure-displacement cohesive elements which model tangential flow within the gap have been used for our analysis (Abaqus Manual 2014). We use a half-symmetry plane strain 2D model to keep the degrees of freedom to a minimum while capturing the most significant physics. For the formation with pore pressure, we used the **CPE4P** elements. For modeling the fluid flow and pressure loss from the surface to the depth of fracture initiation, we use fluid flow elements. The fluid is injected to both the borehole (pore pressure-displacement elements) and fracture plane (CZM with pore pressure elements). A sample model showing the mesh and highlighting the connection between the fluid elements and wellbore can be seen in Figure 2.

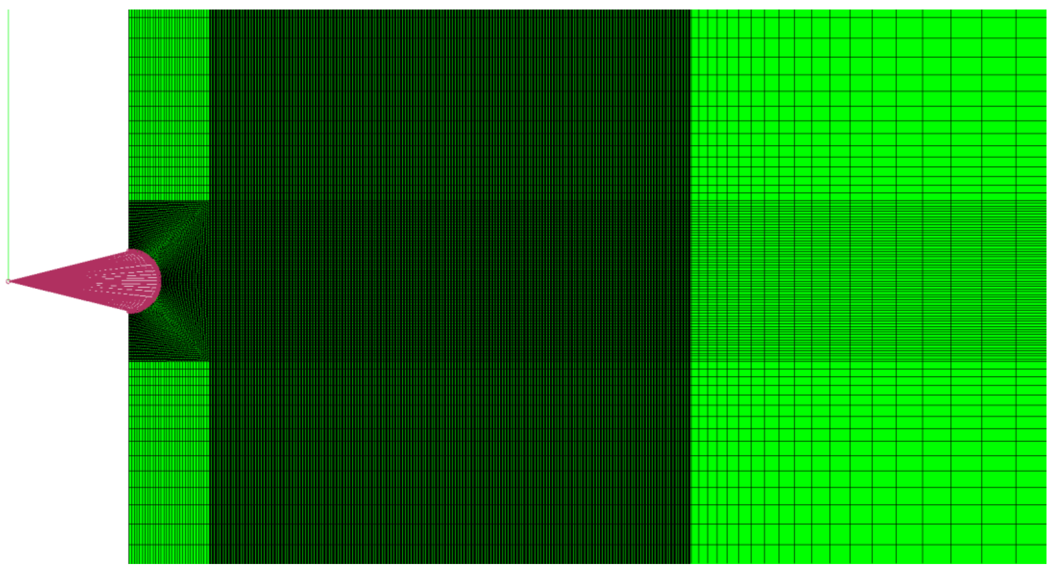

Figure 2. Model mesh

The smaller computational cost of a 2D mesh allows modeling a large number of cases with varying formation and fluid properties. This way we can evaluate the envelope of plausible field scenarios. Finally, we can generate a range of expected values for fracture initiation, and more importantly, the range of fracture geometries created can be studied. This is of great help for drilling, as any materials which can be used for plugging the fractures can be sized and ordered in advance to have ready while drilling. This can also greatly reduce the cost of drilling as it reduces the non-productive time which occurs while waiting on delivery of products once drilling begins.

The model has been benchmarked with known semi-analytical solutions for fracture propagation (Zielonka et al., 2014) and has also been validated with laboratory scale experiments of hydraulic fracturing (Ning et al., 2015).

3. Workflow

The drilling engineer can quickly become familiar with the workflow and start executing the analysis as it allows a separation between the user and the model generation and execution. The process begins with the user filling out a template of material properties for the formation and the fluid. Some of the properties which are not well known in advance can be left blank and empirical models are used internally to estimate them. In addition, it is possible to specify value ranges instead of individual values. For example, if the user specifies three values for Young's modulus and two values for Poisson's ratio, the workflow will generate the input files for all the six combinations. After the input values are specified, all the input files needed are generated automatically. If more than one analysis is needed, the cases are submitted in parallel on a computing cluster. After the Abaqus runs are complete, the results are automatically post-processed using Abaqus post-processing scripts and various graphs of interest to the drilling engineer are generated. The user has direct access to these plots. Advanced users can also access the raw data.

This automated workflow allows a much better use of the engineer's time, as the user spends very little time on preparing and running the analysis, and also allows users who are unfamiliar with Abaqus to perform the task. A schematic illustrating the workflow is shown in Figure 3.

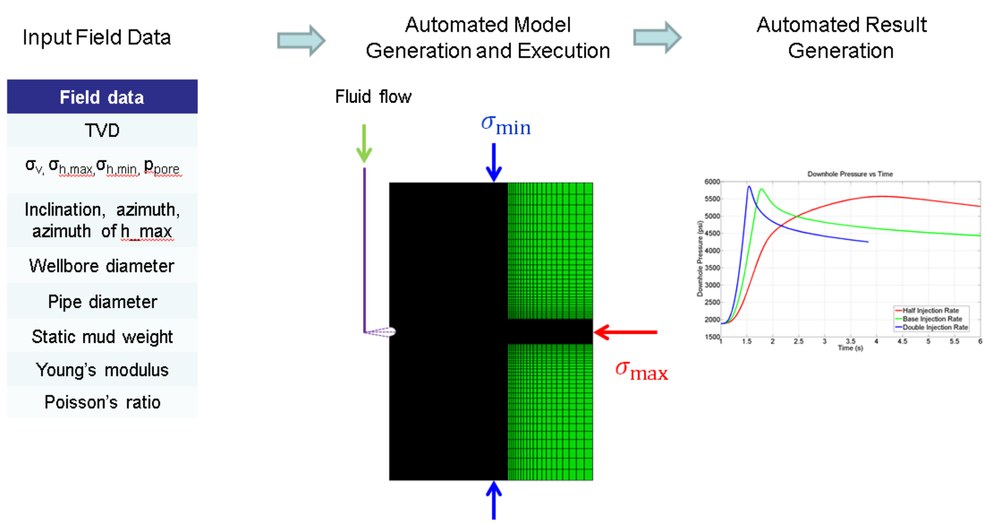

Figure 3. Model generation workflow.

4. Results

Solving for the near-wellbore stresses during dynamic fracture growth provides a wealth of information which was not accessible before. We are able to analyze the width and length evolution of the fracture for a given set of conditions, and also look at the pressure response, the tangential stresses at the wellbore, and the stresses around the fracture tip. In addition, we can model the stresses after the fracture has been arrested and the fluid has diffused into the formation, allowing the pore pressure to return to a level close to its original value. Figure 4 shows the tangential stresses ($\sigma_{\theta\theta}$) around the wellbore after the fracture has grown to some length. Figure 5 shows the pressure response in the wellbore during the fracture initiation and propagation for three different injection rates. This type of plot is automatically generated after the analysis. Figure 6 shows the width evolution at the fracture mouth for these injection rates. Figure 7 shows the length evolution for the same three fractures.

A variety of other data can also be presented which was not possible to gather before, e.g. the time for the fracture to grow to a given length or the dynamic aspect ratio of the fracture. In addition, the value and location of the maximum and minimum tangential stress at the wellbore during fracture evolution can be predicted. Knowing the minimum (least compressive) tangential stress at the wellbore, and how it changes with fracture width and length, allows us to determine the ideal particle size to use for plugging the fracture. In addition, it allows estimating the pressure needed to initiate another fracture.

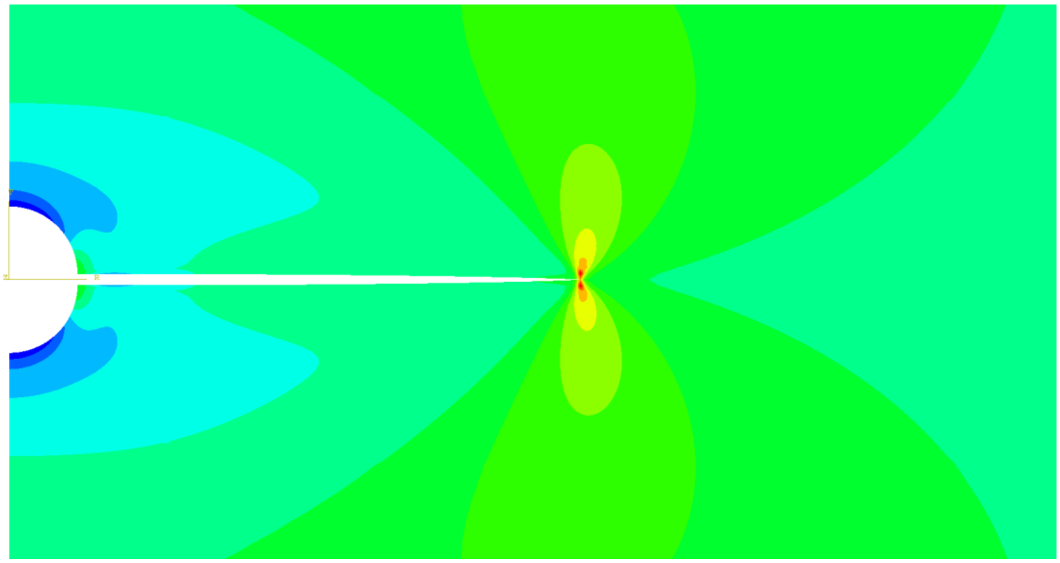

Figure 4. Tangential stress $\sigma_{\theta\theta}$ around the fracture and wellbore. Fracture width exaggerated ten times.

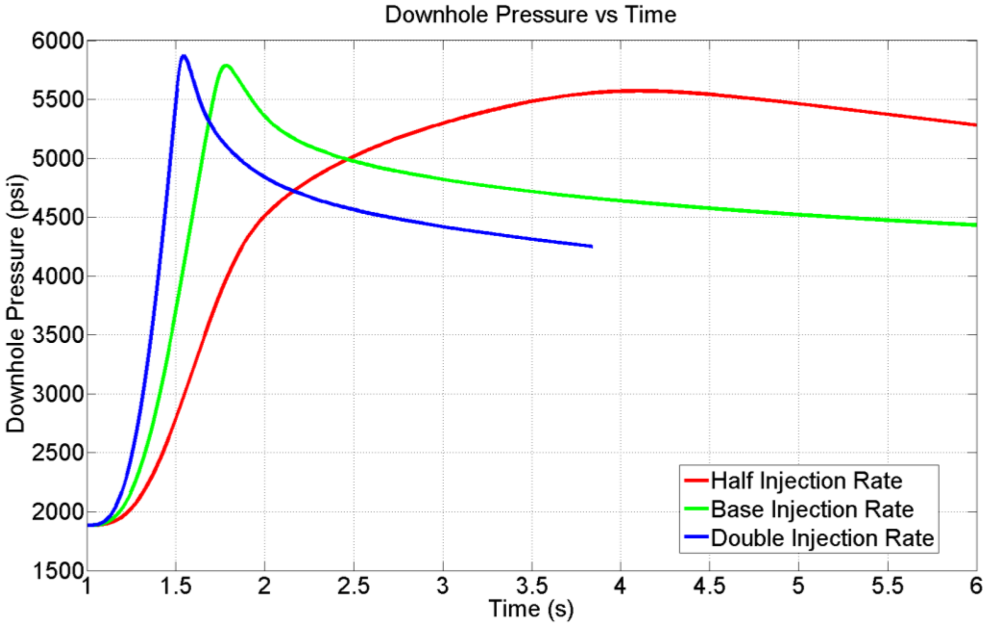

Figure 5. Pressure response for three different injection rates.

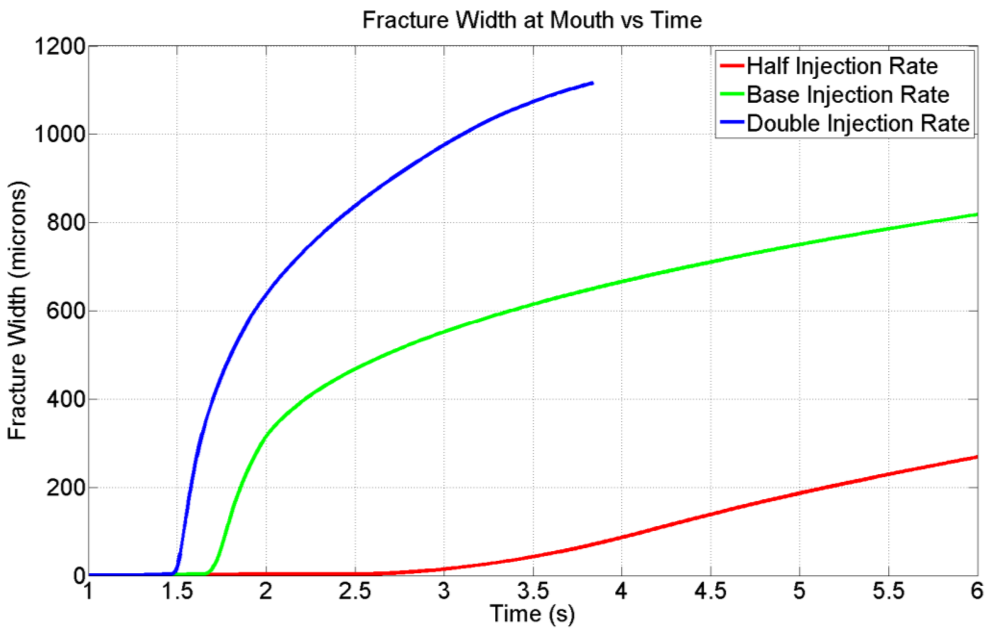

Figure 6. Fracture width at mouth evolution for the three different injection rates.

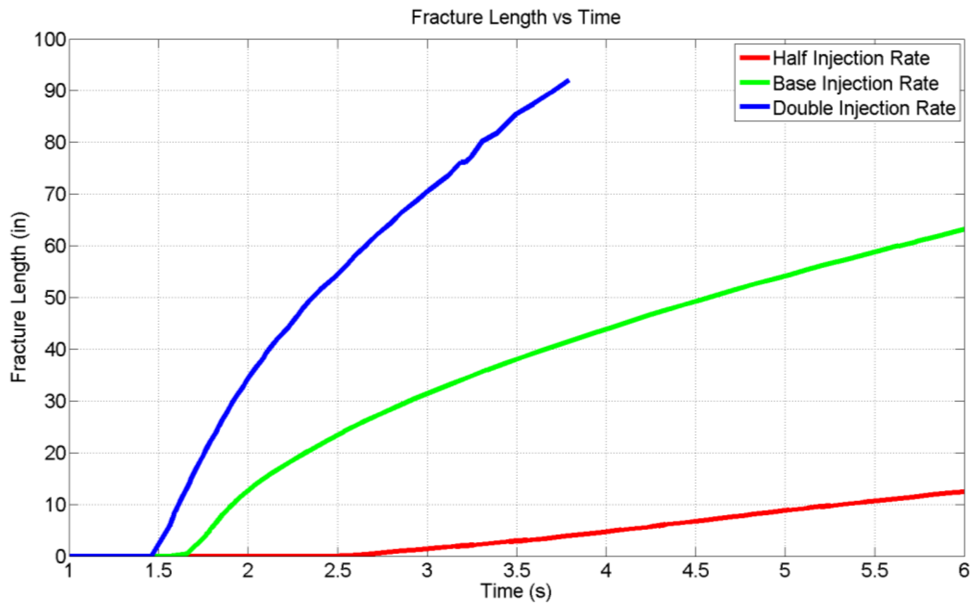

Figure 7. Fracture length evolution for the three different injection rates.

Contrary to some existing models, we are not assuming a given fracture length, but allowing for the fracture to propagate at a width and length combination governed by the complex interaction between rock deformation, fracture fluid pressure, and fluid leak-off.

5. Conclusions

We presented a workflow which allows predicting the particle size needed to plug a dynamically growing fracture. The size is chosen such that it maximizes the wellbore tangential stresses at the wellbore faces. The workflow is based on an automated generation of Abaqus input files from a user supplied list of material properties and field data. The model is generated, executed, and post-processed completely autonomously, minimizing user processing time. It also allows drilling engineers who are not familiar with running Abaqus to be able to perform the analysis.

The fracture modeling captures dynamic fracture growth in a porous formation utilizing CZM elements for the fracture plane. These capabilities, unique to Abaqus, allow for a more accurate prediction of the fracture geometry and the pore pressure dependent transient stresses near the wellbore.

6. References

1. Hubbert, M.K., Willis, D.G. *Mechanics of Hydraulic Fracturing*. Transactions of Society of Petroleum Engineers of AIME, 1957, v. 210, pp. 153-168.
2. Haimson, B., Fairhurst, C. *Initiation and Extension of Hydraulic Fractures in Rocks.* SPE 1710. SPE Third Conference on Rock Mechanics. Austin, Texas, 1967.
3. Ning, J., Kao, G., Kostov, N., Searles, K. H., Buechler, S. R., and Sanz, P. F. *Experimental Validation of Simulation Capabilities for Hydraulic Fractures Propagating in a Porous Medium*. 2015 Simulia Community Conference, Berlin, Germany.
4. Zielonka, M. G., Searles, K. H., Ning, J., and Buechler, S. R. *Development and Validation of Fully-Coupled Hydraulic Fracturing Simulation Capabilities*. 2014 Simulia Community Conference, Providence RI
5. Abaqus 6.13 Online Documentation. April, 2013.

7. Acknowledgement

We would like to thank ExxonMobil Upstream Research Company and ExxonMobil Development Company for permission to publish this material.